

SOME RESULTS IN THE NUMERICAL ANALYSIS OF STRUCTURAL INSTABILITIES

PART II. DYNAMICS

M. KLEIBER (WARSZAWA)

The paper is a direct continuation of the first part, [1], in which the application of the finite element technique to static stability problems was described and illustrated by a number of numerical examples. In this part of the paper some indications on how impulsive loading problems can be numerically analyzed with respect to the stability characteristics of motion are given. A step-by-step algorithm for the time integration of the nonlinear equations of motion is described and applied to different buckling prone structures subjected to uniform step loading of infinite duration.

1. DYNAMIC BUCKLING PROBLEM

The dynamic stability problem can be classified with respect to the loading conditions as follows:

i) Impulsive loading problems—in this class the dynamic stability of structures subjected to step (or other impulsive) loadings of finite or infinite duration is considered.

ii) Parametric resonance problems—a typical example in this class is the initially straight prismatic column whose two ends are simply supported and upon which a periodic axial compressive load is acting. Such a column is known to develop lateral oscillations if its straight-line equilibrium is disturbed. Depending upon the magnitude and the frequency of the pulsating axial load, the linear Hill or Mathieu equation defining the lateral displacement of the column may yield bounded or unbounded values for these displacements.

iii) Circulatory loading problems—this class consists of problems of buckling under stationary circulatory loads, that is, loads not derivable from a potential and not explicitly dependent on time. The dynamic criterion of buckling is useful in the nonconservative static stability analysis of such problems since the commonly static methods of determining critical load can give incorrect results.

iv) Aeroelastic problems—in this class the interaction between the nonconservative aerodynamic forces and the elastic structures is analysed.

The above classification is not fundamental in any sense of the word and simply groups problems that are treated by similar mathematical tools.

The following considerations will be devoted exclusively to impulsive loading problems. Even for such problems only, however, the picture drawn in the previous

part, [1] becomes far more complicated. We accept in the sequel the following definition of the dynamic buckling load, [2].

Consider a structure under time-dependent loading $\mathbf{R} = \lambda f(t) \mathbf{R}_0$ where the time variation $f(t)$ is normalized so that its maximum value is unity. Dynamic buckling for a given $f(t)$ and \mathbf{R}_0 is studied by considering the set of structural responses associated with the set of loading histories $\mathbf{R} = \lambda f(t) \mathbf{R}_0$ generated by various values of λ . The critical value of λ that corresponds to dynamic buckling (as defined later) will be called the dynamic buckling load and will be denoted by λ_D .

It is important to realize that, similarly as in statics, after a structure buckles dynamically it often takes on a stable configuration again, although it cannot be serviceable any longer.

Such a definition of the dynamic buckling load is of no use unless we can meaningfully formulate an effective buckling criterion (as this was the singularity of the tangent stiffness matrix in the static case). Unfortunately, the definition of a reasonable buckling criterion is still a challenging problem. In the case of rotationally symmetric spherical shells subjected to axisymmetric dynamic loading it is useful to differentiate (in analogy to statics!) two different types of buckling:

a) Axisymmetric dynamic buckling

This type of snap-through buckling is possible when the dynamic response in the whole time range of interest is constrained to be axisymmetric and thus any contribution from circumferentially asymmetric modes is precluded. Obviously, for certain shell geometries and loads a purely axisymmetric response can occur naturally without any need for artificial constraints. Unfortunately, the buckling criteria even for such situations are not as well defined as for static buckling and require an evaluation of the transient response of the shell for various load levels. Then, as a practical criterion, it is often assumed that an axisymmetric structure undergoing an axisymmetric deformation becomes unstable when a slight increase in the magnitude of the load produces a sharp increase in the (axisymmetric) response. Thus the criterion in most common use is based on the plot of the peak (local maxi-

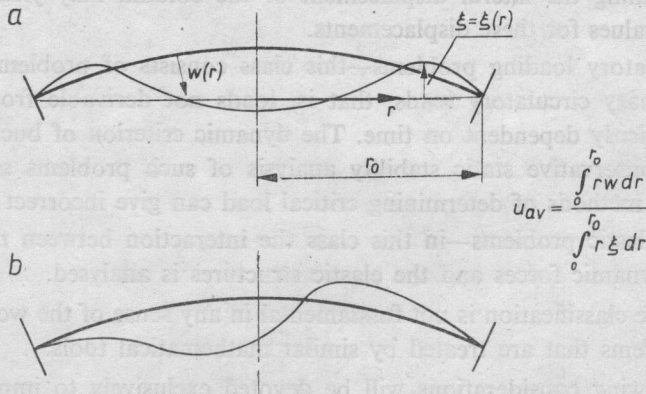


FIG. 1. Dynamic buckling behaviour of a spherical cap.

mum) apex displacement $u_0^{(1)}$ in the whole time interval versus the load amplitude λ . For practical reasons the peak displacement is normally determined on the basis of the structural response within a certain limited time interval $[0, t^*]$. It must therefore be emphasized that even if the applied load is not sufficient to cause snap-through on the first cycle of the response, it can do it later so that in general even the first several displacement peaks do not have to be necessarily representative of the critical behaviour investigations.

The above definition of axisymmetric dynamic snap-through buckling was first suggested in [2] and then used for the analysis of elastic shells by other investigators, cf. [3-9], for instance.

b) Asymmetric dynamic buckling

The second type of buckling, referred to as the asymmetric dynamic buckling, arises when the dynamic response is not constrained or inclined to be symmetric. If the load amplitude reaches some critical value, the shell response can be characterized by a significant growth of the asymmetric displacements which ultimately reach proportions that must be considered as buckling instability. As discussed in [6] for instance, there is at present no well understood and generally accepted criterion available for the asymmetric dynamic buckling of shells. The existing numerical results, although very few, are not in good agreement as compared to each other and, also, to the available experimental results [6]. The way out would be, of course, to consider nonaxisymmetric imperfections and to pursue bifurcation analysis similar to that widely used in static stability problems. However, this means carrying out many times a complete transient analysis with different imperfection patterns corresponding to different Fourier harmonics and can turn out to be very time consuming.

It is commonly hypothesized that bifurcation pressure will not necessarily lead to immediate (asymmetric!) snap-through buckling. However, oscillations corresponding to the secondary, bifurcated asymmetric motion may significantly influence (e.g. accelerate) the occurrence of the snap-through. The shell will then jump over asymmetrically to the reversed position implying further small oscillations of presumably axisymmetric character. In this sense the critical dynamic bifurcation load can be treated as a lower bound to the asymmetric dynamic snap-through load.

All the above hypothetical considerations can be assembled in one diagram as presented in Fig. 2. The figure has a symbolic character and is hypothesized to play a similar role in structural dynamics as Fig. 3 of [1] does in structural statics. The most limiting factor in interpreting the dynamic structural behaviour in accordance

(¹) Sometimes the nondimensional average displacement u_{av} was used being defined as

$$u_{av} = \frac{\int_0^a r w dr}{\int_0^a r \xi dr},$$

where ξ , r , w and a are defined in Fig 1. The numerator is here the volume generated by the shell deformation while the denominator is the constant volume under the cap in the initial position.

with Fig. 2 is the one-degree-of-freedom description of the shell motion—for the description of asymmetric bifurcation modes the use of other displacement-type parameters may appear mandatory.

From Fig. 2 it is seen that the inclusion of time as the additional variable results in the replacement of: i) the static primary (fundamental) equilibrium path by a primary (fundamental) dynamic equilibrium surface S_f , ii) the static secondary (asymmetric) equilibrium path by a secondary (asymmetric) dynamic equilibrium surface S_b , iii) the static bifurcation point by a dynamic bifurcation curve P , $P = S_f \cap S_b$. We emphasize that Fig. 2 describes the ideal structure behaviour under step loading of infinite duration. In the case of an imperfect structure the shell dynamic behaviour can be described in general terms in analogy to the known static concepts.

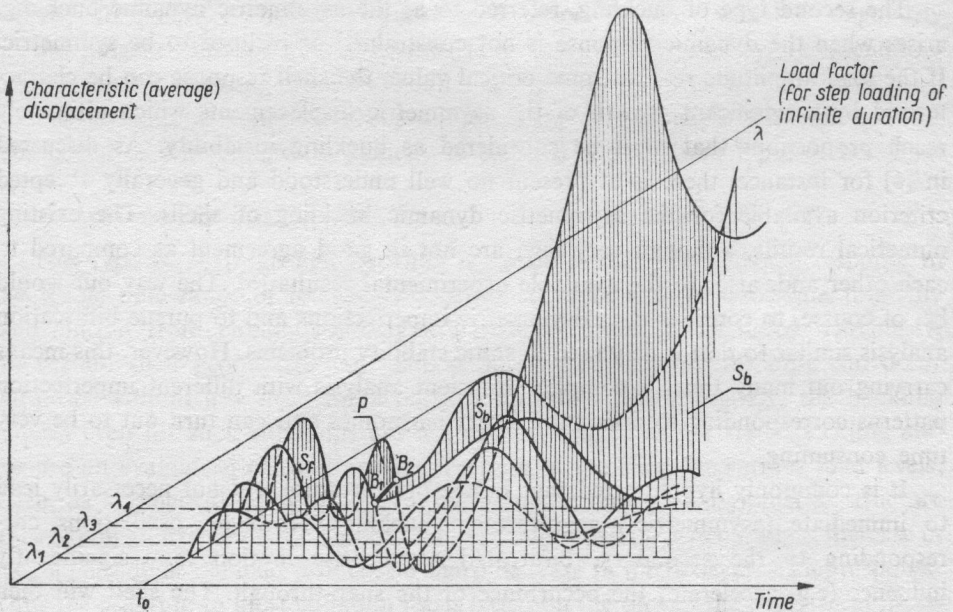


FIG. 2. Dynamic buckling of a cap.

All the numerical calculations to be presented below have been carried out by using a step-by-step algorithm applied to the incremental matrix equation of the nonlinear structural dynamics in the form

$$(1.1) \quad \mathbf{M} \Delta \ddot{\mathbf{r}} + \mathbf{K}_t \Delta \mathbf{r} = \Delta \mathbf{R},$$

where \mathbf{M} is the mass matrix, \mathbf{K}_t is the stiffness matrix at time t (consisting of the constitutive, the initial stress and the initial displacement stiffness matrices) and $\Delta \ddot{\mathbf{r}}$ is the vector of nodal incremental accelerations. In Eq. (1.1) we did not include damping effects but this can be done easily providing the damping matrix can be constructed. Equation (1.1) is usually applied in a slightly modified form to read

$$(1.2) \quad \mathbf{M} \ddot{\mathbf{r}} + \mathbf{K} \mathbf{r} = \mathbf{P} - \mathbf{F}$$

where $\ddot{\mathbf{r}}_{t+\Delta t}$ is the vector of nodal accelerations corresponding to time $t+\Delta t$, $\mathbf{R}_{t+\Delta t}$ is the vector of nodal external loads at time $t+\Delta t$, \mathbf{F}_t is the generalized internal nodal force vector corresponding to time t , e.g.

$$(1.3) \quad \mathbf{F}_t = \mathbf{R}_t - \mathbf{M}\ddot{\mathbf{r}}_t$$

and the following relation was used:

$$(1.4) \quad \Delta\ddot{\mathbf{r}} = \ddot{\mathbf{r}}_{t+\Delta t} - \ddot{\mathbf{r}}_t.$$

Various explicit and implicit time integration methods are presently applied. We used the latter approach in the form of the trapezoidal rule based upon the assumptions

$$(1.5) \quad \dot{\mathbf{r}}_{t+\Delta t} = \dot{\mathbf{r}}_t + \frac{\Delta t}{2} (\ddot{\mathbf{r}}_{t+\Delta t} + \ddot{\mathbf{r}}_t), \quad \mathbf{r}_{t+\Delta t} = \mathbf{r}_t + \frac{\Delta t}{2} (\dot{\mathbf{r}}_{t+\Delta t} + \dot{\mathbf{r}}_t).$$

Using Eqs. (1.5) and the relation

$$(1.6) \quad \Delta\mathbf{r} = \mathbf{r}_{t+\Delta t} - \mathbf{r}_t,$$

Eq. (1.2) gives

$$(1.7) \quad \left(\mathbf{K}_t + \frac{4}{(\Delta t)^2} \mathbf{M} \right) \Delta\mathbf{r} = \mathbf{R}_{t+\Delta t} - \mathbf{F}_t + \mathbf{M} \left(\frac{4}{\Delta t} \dot{\mathbf{r}}_t + \ddot{\mathbf{r}}_t \right).$$

Equation (1.7) is solved recursively for all time steps. As Eqs. (1.2) and (1.7) are derived here by linearizing the response about the configuration at time t , the Newton-Raphson iteration scheme was used to reduce the linearization error.

2. NUMERICAL ANALYSIS OF DYNAMIC INSTABILITIES

The aim of calculations reported in the present section was to carry out the dynamic analysis of some complex structures and to investigate their behaviour under critical loading conditions. With these results we also hope to be able, at least partially, to substantiate our fundamental hypothesis concerning dynamical structural behaviour laid down in the previous section.

We have so far discussed the critical dynamic behaviour of structures which possess a certain degree of symmetry so that one can talk of the bifurcation phenomena. We start by describing numerical results obtained for the elastic and the elastic-plastic cap problem.

The analysis here followed exactly the pattern described in [1] for the case of statics. The broken and solid lines shown in Fig. 3 are taken as "weighted averages" of the results reported in [2-9]. We analysed the same shell configurations and the similar concept of imperfection analysis was taken advantage of. The only differences were now the inclusion of inertia effects and the necessity of performing in each case a whole series of numerical computations as described in the previous section. The fact that the numerical analysis for each run was confined to a certain time interval only (3 to 4 response peaks on the average) imposes certain limitations on the accuracy of the results.

The way the results are presented in the same as in [1], cf. Fig. 7 of [1]. The reduction of the critical loads in the case of elastic-plastic shells is clearly seen. The bifurcation loads obtained in both elastic and inelastic analyses were obviously somewhat lower than the asymmetric dynamic snap-through buckling loads. For a more detailed analysis of this research project the reader is referred to forthcoming papers.

As a next example we take the space truss structure discussed in [1]. We shall discuss first the dynamic behaviour of the ideal elastic truss. The structure is subjected to uniform step loading of infinite duration in the form of a concentrated force applied to the node 1.

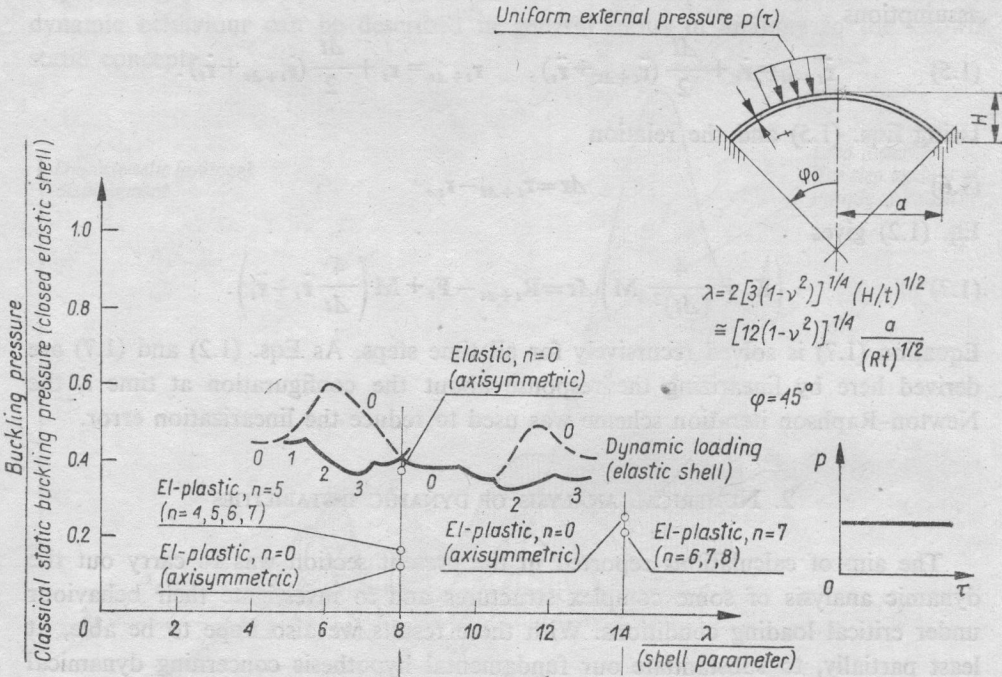


Fig. 3. Dynamic buckling pressures for elastic clamped shallow spherical shells.

The magnitude of the load is varied and the response (the node 1 vertical displacement as a function of time) is observed. In Fig. 4 a few responses as this are shown in a certain time interval for different load magnitudes. It is noticed that at some load level (between 500 kG and 600 kG) the response increases dramatically with a relatively small increase in load. The more detailed investigations show, Fig. 5, that the dynamic snap-through load value is about 513.00 kG. It is seen, however, that had we confined ourselves to the time interval [0, 10 ms], the buckling load would have been identified as 513.25 kG. This is so because the significant growth of the response under the load 513.00 kG is induced after more than 50 ms. This illustrates the general rule formulated before that the first several displacement peaks do not have to be necessarily representative of the critical behaviour investigations. The plot of maximum displacements (independent of time at which

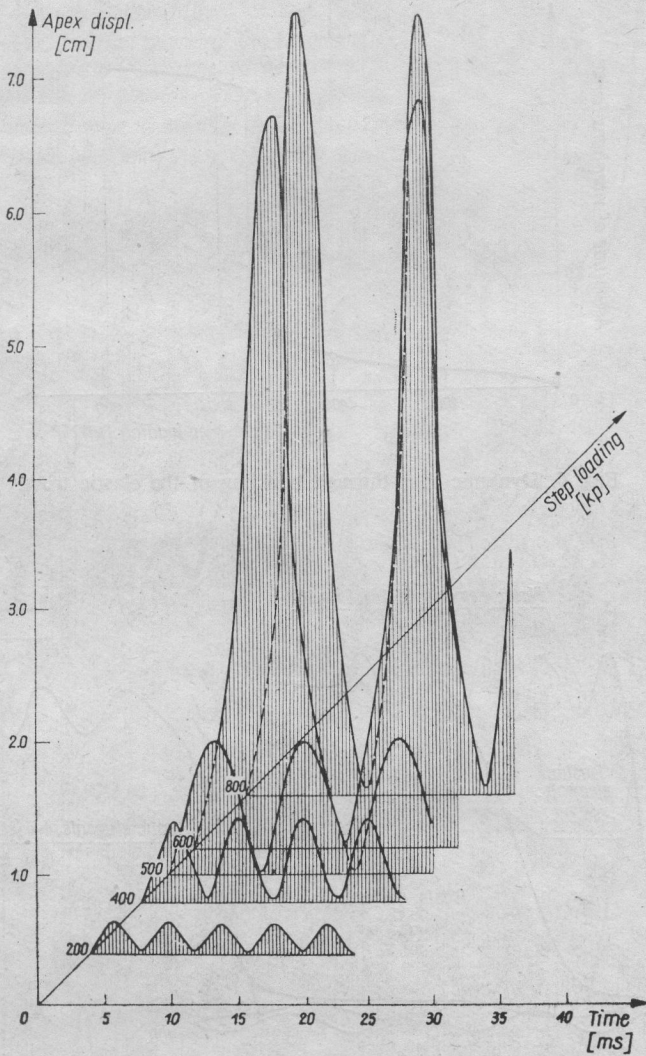


FIG. 4. Dynamic buckling behaviour of the elastic truss.

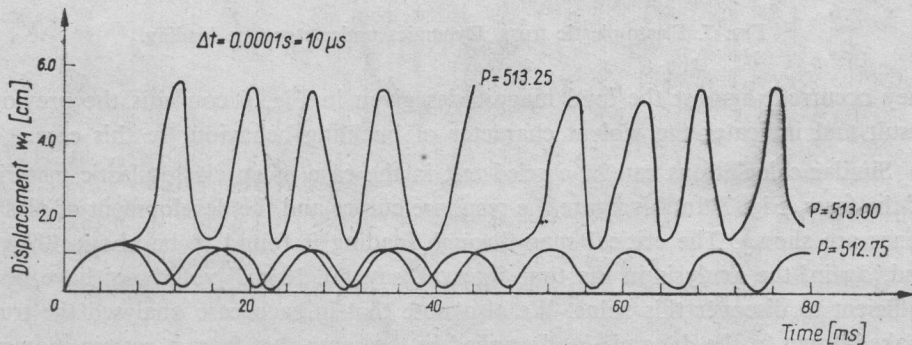


FIG. 5. Dynamic snap-through buckling of the elastic truss.

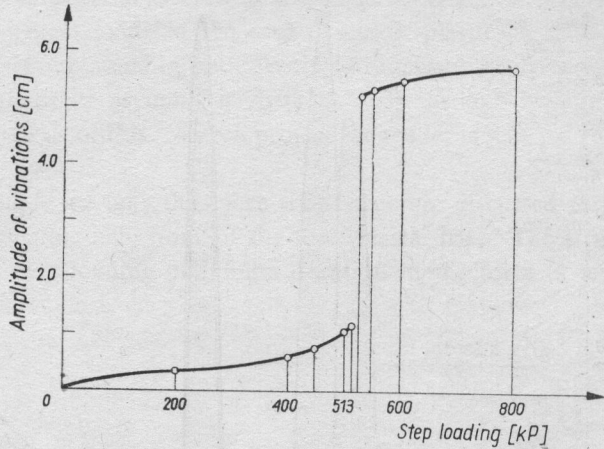


FIG. 6. Dynamic snap-through buckling of the elastic truss.

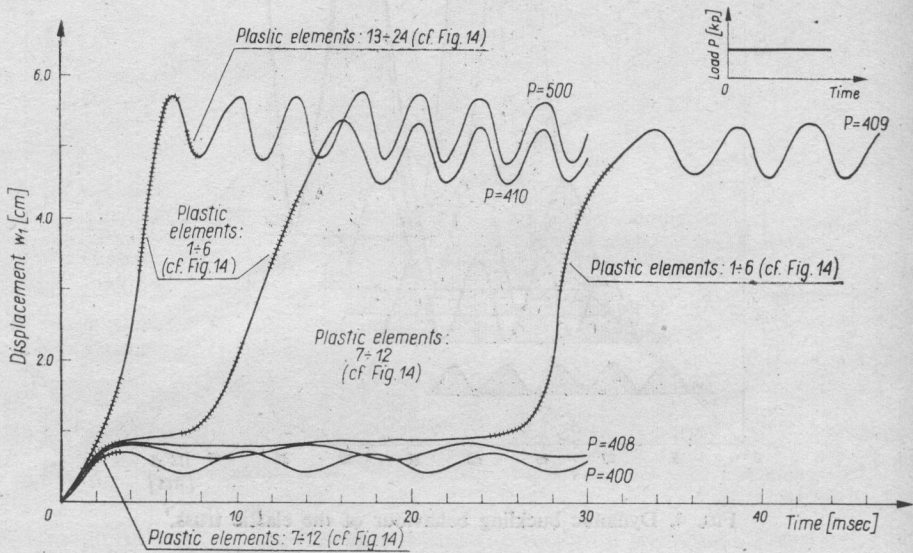


FIG. 7. Elasto-plastic truss. Dynamics under step-type loading.

they occurred) against the load magnitudes given in Fig. 6 confirms the previous result and indicates the violent character of buckling behaviour in this case.

Similar calculations can be carried out in the case of an elasto-plastic material of the truss, Fig. 7. In this figure the response curves and the development of plastic zones are shown. The critical snap-through loading is found to be about 409 kG and, again, the analysis in the time interval, say, $[0, 10 \text{ ms}]$ would not have been sufficient to discover this value. We also note that in each case analysed the truss shaked-down to the dynamic load applied in the sense that from a certain moment further response was purely elastic.

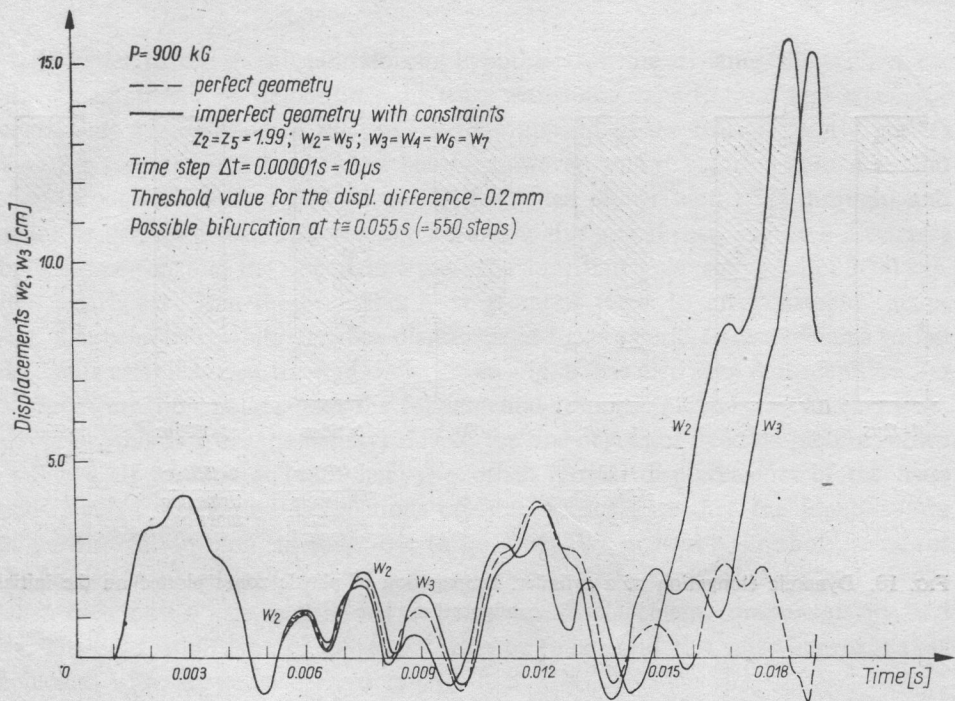


FIG. 8. Dynamics of the elastic truss.

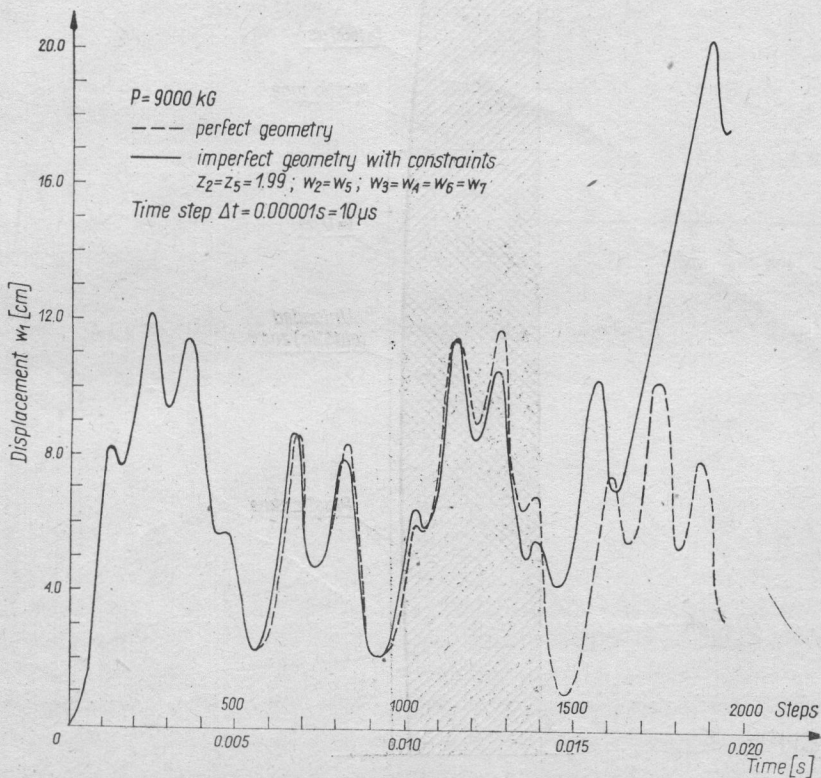


FIG. 9. Dynamics of the elastic truss.

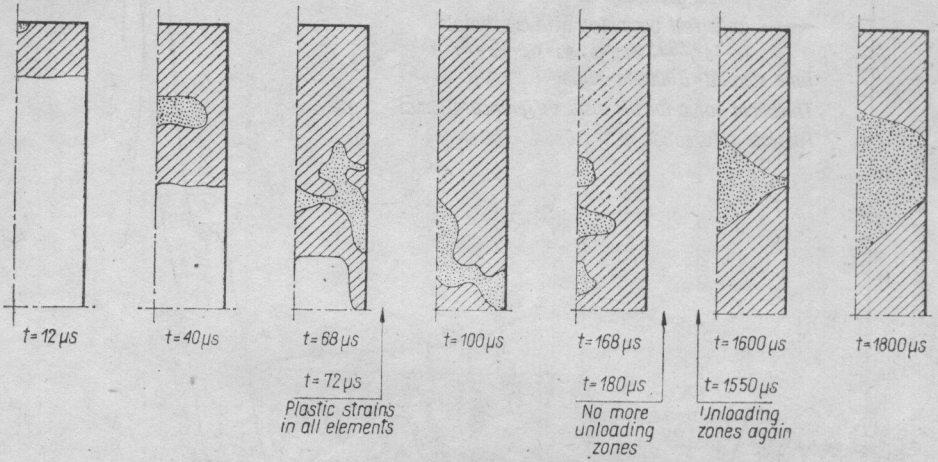


FIG. 10. Dynamic elongation of a cylinder. Propagation of plastic zones plotted on the initial configuration.

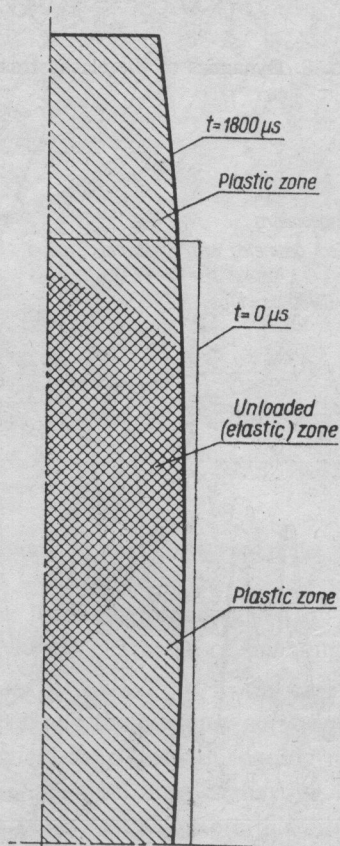


FIG. 11. Deformed configuration at the final stage of deformation.

In order to try to substantiate our hypothesis on the dynamic bifurcation behaviour of structures, we consider the truss with some imperfections and kinematic constraints as described in Fig. 8. The load applied to the truss is clearly greater than the snap-through load found before; however, this structure admits a second snap-through instability, Fig. 14 of [1] (for much higher load level through) and a similar behaviour can also be expected in the dynamical case. Figure 8 illustrates both the perfect and the imperfect truss behaviour under the step load of 9000 kG. It is clearly seen that the imperfect truss geometry leads to an "unstable" snap-through behaviour while the apex displacement for the perfect truss remains within the limits established at the first cycle. From Fig. 8 it is also seen that identification of the bifurcation point along the fundamental response curve is not an easy task. However, this is (perhaps mainly) due to the one-degree-of-freedom picture shown in Fig. 8. If we look at Fig. 9 here two other vertical displacements of the truss nodes 2 and 3 are plotted as functions of time, we shall see that the identification of the bifurcation moment turns out to be easier. We present a threshold value for the displacement difference as 0.2 mm and start to draw three lines instead of one when such a difference is achieved between the displacement components w_2 and w_3 . The bifurcation time of about 5.4 ms was found and this value approximately coincides with the value derived in Fig. 8.

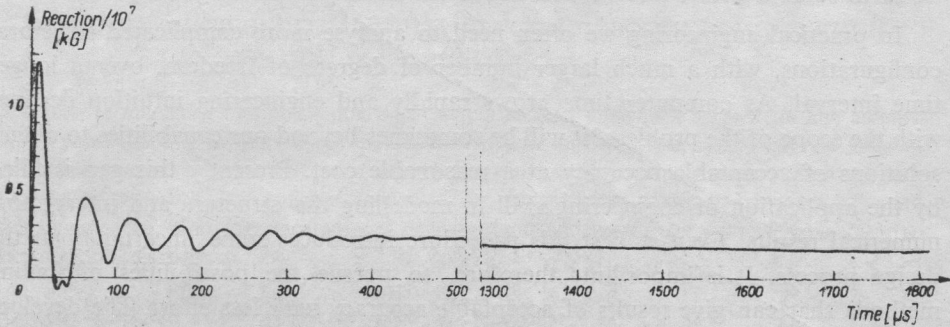


FIG. 12. Dynamic elongation of a cylinder.

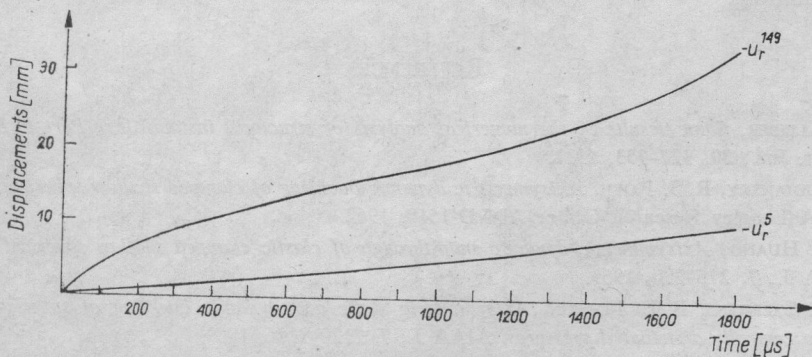


FIG. 13. Dynamic elongation of a cylinder.

As the last example we present the results obtained in the course of the dynamic analysis of the cylindrical specimen given in Fig. 20 of [1]. The aim of the calculations was to check whether the necking-type behaviour visible under static load conditions can also be observed during dynamic analysis. The specimen was loaded by prescribing the constant velocity of 75 m/s in the z -direction at the boundary points 145-149, Fig. 20 of [1]. The development of plastic zones is shown in Fig. 10, 11 the typical pattern known from statics is here to some extent reproduced with plasticity gradually spreading out over the whole specimen, fully plastic behaviour over the long time interval and initiation of unloading in some limited parts of the specimen afterwards. However, in contrary to the static behaviour no instability effects can be attributed to such an unloading. Figures 11, 12 and 13 show clearly that the continuing deformation process is stable and no necking phenomenon appears.

CONCLUSIONS

From the analysis of this and the first part [1] of the study it is seen that an approach to structural stability analysis which could be called "direct" may yield a lot of interesting informations concerning the critical behaviour of structures. However, most of the methods developed so far may be used effectively only if we have some a priori information about the nature of the singular points.

In practical engineering we often need to analyse more complicated structural configurations, with a much larger number of degrees of freedom, over a longer time interval. As computer time grows rapidly and engineering intuition declines with the scope of the problem, it will be sometimes beyond our capabilities to obtain solutions of acceptable accuracy at a reasonable cost. Presently this gap is filled by the application of engineering skill in modelling the structure and interpreting numerical results. Even at best this procedure introduces some uncertainty in the design process. It is important, therefore, to pursue the possibilities of finding methods that can give results of acceptable accuracy with less effort. The development of these must be based upon better understanding of the buckling phenomena. It is hoped that the results presented in the paper will contribute to such a better understanding.

REFERENCES

1. M. KLEIBER, *Some results in the numerical analysis of structural instabilities, Part I. Statics*, Rozpr. Inž., **30**, 327-353, 1982.
2. B. BUDIANSKY, R. S. ROTH, *Axisymmetric dynamic buckling of clamped shallow spherical shells*, NASA Langley Research Center, TN D-1510, 1962.
3. N. C. HUANG, *Axisymmetric dynamic snap-through of elastic clamped shallow spherical shells*, AIAA J., **7**, 215-220, 1969.
4. W. B. STEPHENS, R. E. FULTON, *Axisymmetric static and dynamic buckling of spherical caps due to centrally distributed pressures*, AIAA J., **7**, 2120-2126, 1969.
5. J. A. STRICLIN, J. E. MARTINEZ, *Dynamic buckling of clamped spherical caps under step pressure loadings*, AIAA J., **7**, 1212-1213, 1969.

6. N. AKKAS, *Bifurcation and snap-through phenomena in asymmetric dynamic analysis of shallow spherical shells*, *Comp. Struct.*, **6**, 241-251, 1976.
7. R. E. BALL, J. A. BURT, *Dynamic buckling of shallow spherical shells*, *J. Appl. Mech.*, **40**, 411-416, 1973.
8. R. KAO, N. PERRONE, *Dynamic buckling of axisymmetric spherical caps with initial imperfections*, *Comp. Struct.*, **9**, 463-473, 1978.
9. M. H. LOCK, S. OKUBO, J. S. WHITTIER, *Experiments on the snapping of a shallow dome under a step pressure load*, *AIAA J.*, **6**, 1320-1326, 1968.

STRESZCZENIE

PRZYKŁADY NUMERYCZNEJ ANALIZY NIESTATECZNOŚCI KONSTRUKCJI
CZĘŚĆ II. DYNAMIKA

W pracy podano szereg przykładów zastosowania metody elementów skończonych do analizy utraty stateczności sprężystych i niesprężystych układów konstrukcyjnych poddanych obciążeniom dynamicznym. Opisano algorytm całkowania dyskretyzowanych równań ruchu i zastosowano go do oceny dynamicznych obciążeń krytycznych szeregu konstrukcji. Sformułowano hipotezę dotyczącą bifurkacyjnego zachowania się układów poddanych obciążeniom dynamicznym.

Резюме

ПРИМЕРЫ ЧИСЛЕННОГО АНАЛИЗА НЕУСТОЙЧИВОСТИ КОНСТРУКЦИЙ
Ч. II. ДИНАМИКА

В работе приведен ряд примеров применения метода конечных элементов для анализа потери устойчивости упругих и неупругих конструкционных систем, подвергнутых динамическим нагрузкам. Описан алгоритм интегрирования дискретизированных уравнений движения и он применен для оценки динамических критических нагрузок ряда конструкций. Сформулирована гипотеза, касающаяся бифуркационного поведения систем, подвергнутых динамическим нагрузкам.

POLISH ACADEMY OF SCIENCES
INSTITUTE OF FUNDAMENTAL TECHNOLOGICAL RESEARCH

Received August 13, 1981.